University of South Carolina
Scholar Commons

Faculty Publications | Chemical Engineering, Department of

2002

Study of Sn-Coated Graphite as Anode Material for Secondary Lithium-Ion Batteries

Basker Veeraraghavan
University of South Carolina - Columbia

Anand Durairajan
University of South Carolina - Columbia

Bala Haran
University of South Carolina - Columbia

Branko N. Popov
University of South Carolina - Columbia, popov@engr.sc.edu

Ronald Guidotti

Follow this and additional works at: https://scholarcommons.sc.edu/eche_facpub

 Part of the Chemical Engineering Commons

Publication Info

Journal of the Electrochemical Society, 2002, pages A675-A681.
© The Electrochemical Society, Inc. 2002. All rights reserved. Except as provided under U.S. copyright law, this work may not be reproduced, resold, distributed, or modified without the express permission of The Electrochemical Society (ECS). The archival version of this work was published in the Journal of the Electrochemical Society.
http://www.electrochem.org/
Publisher's link: http://dx.doi.org/10.1149/1.1470653
DOI: 10.1149/1.1470653

This Article is brought to you by the Chemical Engineering, Department of at Scholar Commons. It has been accepted for inclusion in Faculty Publications by an authorized administrator of Scholar Commons. For more information, please contact digres@mailbox.sc.edu.

Journal of The Electrochemical Society, **149** (6) A675-A681 (2002)
0013-4651/2002/149(6)/A675/7/$7.00 © The Electrochemical Society, Inc.

Study of Sn-Coated Graphite as Anode Material for Secondary Lithium-Ion Batteries

Basker Veeraraghavan,[a] Anand Durairajan,[a,*] Bala Haran,[a,] Branko Popov,[a,**,z] and Ronald Guidotti[b,**]**

[a]*Department of Chemical Engineering, University of South Carolina, Columbia, South Carolina 29208, USA*
[b]*Sandia National Laboratories, Albuquerque, New Mexico, USA*

Tin-graphite composites have been developed as an alternate anode material for Li-ion batteries using an autocatalytic deposition technique. The specific discharge capacity, coulombic efficiency, rate capability behavior, and cycle life of Sn-C composites has been studied using a variety of electrochemical methods. The amount of tin loading and the heating temperature have a significant effect on the composite performance. The synthesis conditions and Sn loading on graphite have been optimized to obtain the maximum reversible capacity for the composite electrode. Heating the composite converts it from amorphous to crystalline form. Apart from higher capacity, Sn-graphite composites possesses higher coulombic efficiency, better rate capability, and longer cycle life than the bare synthetic graphite. Current studies are focused on reducing the first cycle irreversible capacity loss of this material.
© 2002 The Electrochemical Society. [DOI: 10.1149/1.1470653] All rights reserved.

Manuscript submitted May 31, 2001; revised manuscript received December 23, 2001. Available electronically April 12, 2002.

To ensure long cycle life and safety, different types of carbon including graphite[1] and coke[2] have been studied as anodes for the Li-ion battery. Carbon based anodes have many desirable properties like high capacity, low and flat potential profile for lithium intercalation, and low cost. In theory, carbon anodes can intercalate with lithium in the ratio 1:6, forming the compound LiC_6, with a capacity of 372 mAh/g.[3] However, it is generally difficult to obtain such high theoretical capacity. For commercial applications, mesocarbon microbeads (MCMBs) are the anodes of choice and it gives a reversible discharge capacity of 300 mAh/g. Present attempts are focused on developing cheaper alternatives to MCMB with similar capacity and cycling behavior.

Recently, alternate anode materials based on Sn have received tremendous attention due to their high theoretical capacity. Tin alloys extensively with lithium,[4] forming various Li_xSn_y type compounds giving rise to a theoretical capacity of 991 mAh/g. However, tin, when used alone as an anode material, loses capacity rapidly. The reason for this is the large volume change associated with the formation of different Li-Sn phases.[5] Tin expands as much as 259% when alloying with lithium.[5] During cycling, this large expansion and contraction leads to disintegration of the anode material, thereby resulting in rapid capacity decay during normal cycling. It has been suggested that reducing the particle size of the Li^+ storage material or reducing the extent of alloying may improve the situation.[5] Whitehead *et al.*[6] have shown that reducing the particle size of Sn leads to better reversibility. Li and Martin[7] have used sol-gel template synthesis to prepare thin films of SnO_2 nanofibers, which show very high capacity and better capacity retention, even at high discharge rates. On the other hand, Idota *et al.*[8] have shown that amorphous Sn-based materials show better cycling behavior. In general, present research is focused on developing amorphous Sn particles with small particle size.

Combining the high capacity of tin with the good cycling behavior of carbon can yield promising results. Using this approach, Li *et al.*[9] have used chemical precipitation of Sn on graphite to synthesize Sn-C composites. However, the discharge capacity of their composite shows significant fading on cycling. We have previously developed an electroless deposition technique for depositing Ru,[10] Ni,[11] and Pd[12] on carbon. This approach is both economical and efficient for loading finely structured amorphous particles onto pretreated substrates. By electroless deposition, it is possible to load amorphous tin particles on graphite.

The objective of this work is to develop superior graphite composite anodes for Li-ion cells by electrocatalytic inclusion of amorphous Sn on graphite. To achieve this goal we use electroless deposition of tin as a surface modification treatment to improve the discharge capacity and reaction kinetics of the graphite anode. Next, the synthesis conditions and Sn loading on graphite have been optimized to obtain the maximum reversible discharge capacity. Finally, extensive material and electrochemical characterization has been done to characterize the Sn-C composite performance as a Li-ion anode material.

Experimental

Composite synthesis.—Synthetic graphite, commercially known as SFG10, was used as received from Timcal America for all the experimental studies. Sn particles were embedded on the host graphite surface by using an electrocatalytic process. The substrates were pretreated in a reducing hypophosphite bath. Tin coating was carried out at 50-60°C for 0.5 h from an alkaline bath containing 6.38 g/L $SnCl_2$ in 38 g/L NaOH. Sodium hypophosphite (8 g/L) was used as the reducing agent and sodium citrate (30.8 g/L) served as the complexing agent for the autocatalytic reduction process. Altering the $SnCl_2$ concentration in the plating bath varied the amount of tin loading on graphite. After the completion of the deposition process, the concentration of tin in the plating bath was analyzed by titration.[13] This helped in estimating the amount of tin dispersed on the graphite surface. Composites with four different Sn contents were obtained −5, 10, 15, and 20% (by weight).

Material characterizations.—The morphology and the surface compositions of the bare coated graphite were analyzed using a Hitachi S-2500 delta scanning electron microscope. The effect of heating on the crystallinity of the deposit was analyzed using Rigaku D/Max-2200 powder X-ray diffractometer (XRD) using Bragg-Brentano geometry with Cu Kα radiation. Thermogravimetric analysis (TGA) was done to determine change in sample weight with increase in temperature. Changes in the graphite surface area due to tin inclusion were studied using Micromeritics Pulse Chemisorb 2700, based on a single-point, Brunauer-Emmett-Teller (BET) method. Each sample was dried in a flowing stream of argon at 200°C for 1 h prior to BET measurement.

Electrode preparation and electrochemical characterization.—Typical graphite negative electrodes were prepared by adding 10% liquid polytetrafluoroethylene (binder, Aldrich brand) and 50% (v-v) solution of isopropyl alcohol (solvent). The resulting slurry was then mixed in an ultrasonic cleaner for 1 h. Pellets of the finely mixed metal encapsulated carbon samples were prepared by the cold-rolling technique. Disk electrodes, 1.4 cm^2 in area, were cut

* Electrochemical Society Student Member.
** Electrochemical Society Active Member.
z E-mail: popov@engr.sc.edu

Downloaded 28 Jul 2011 to 129.252.86.83. Redistribution subject to ECS license or copyright; see http://www.ecsdl.org/terms_use.jsp

from the cold pressed material. Since the graphite is coated with tin, no additional conducting additives were added during the electrode preparation for the composite. Electrochemical characterization studies were performed using a three-electrode T-cell setup. T cells were prepared in a glove box filled with ultrapure argon (National Gas and Welders Inc.). The electrodes in the T cells were prepared by cold pressing material on both sides of metal current collectors (MS cylinders). Pure lithium metal was used as the counter and reference electrode. 1 M $LiPF_6$ was used as the electrolyte in a 1:1 mixture of ethylene carbonate (EC) and dimethyl carbonate (DMC) with less than 15 ppm H_2O and 80 ppm HF (EM Inc.). A Whatman fiber membrane (Baxter Diagnostic Co.) was used as a separator. More details about the preparation of this type of Li-ion cells can be found elsewhere.[14]

Cycling and rate capability studies were carried out using an Arbin battery test station (BT-2043) at a low current density of 0.1 mA/cm^2 (~C/15 rate), with the cutoff potentials of 0.005 and 2 V *vs.* Li/Li^+. In this paper, the discharge capacity of the negative electrode refers to the lithium intercalation capacity while the charge capacity refers to the lithium deintercalation capacity. Cyclic voltammograms (CVs) were obtained at a scan rate of 0.05 mV/s using EG&G potentiostat (model 273A). Impedance studies were performed using a Solartron 1255 analyzer along with an EG&G potentiostat (model 273A) over a frequency range of 100 kHz to 1 mHz with a signal amplitude of 5 mV, peak to peak.

Results and Discussion

Material characterization.—Scanning electron microscopy and energy dispersive analysis by X-ray (SEM and EDAX) studies.—

SEM studies were performed to check the dispersion of tin over the graphite substrates. Figure 1 shows the SEM pictures for Sn composite graphite sample. The SEM micrograph of bare graphite is also shown for comparison. As seen from the SEM pictures, autocatalytic deposition of tin leads to dispersion of fine particles of Sn on the flake-like host graphite structure (shown by bright spots). Spot analysis by EDAX on these bright regions confirmed the presence of tin. Figure 2 shows the EDAX analysis of the bare and 15% Sn-coated graphite. The plot clearly shows the appearance of new peaks for tin, which is not initially present for the bare graphite.

Crystalline structure.—According to Courtney and Dahn,[5] Sn oxide forms a reversible Li anode because of the formation of Lithium oxide during the first cycle. The Li_2O acts as a matrix, which keeps the electrode particles mechanically connected together. The oxygen content of the tin oxide will be critical in determining the irreversible capacity of the composites. In our case, the composite after deposition contains Sn deposited in the form of $Sn(OH)_2$ and $Sn(OH)_4$. This when heated gets converted itself to SnO and SnO_2 by losing water. The SnO and SnO_2 thus formed can be either amorphous or crystalline in nature depending on the heating temperature. Hence, it is essential to heat the composite to remove the water and also to convert the Sn to an oxide. Sn, a low melting element with a melting point of 232°C, has lower temperatures of recrystallization as compared to other metals. Heating the Sn deposit to 300 and 400°C can thus change the morphology and distribution, and could be a cause for changing the Sn utilization in these composites. Therefore the physical and electrochemical characteristics of the deposit depend largely on the heat-treatment temperature. For one particular loading (15% Sn on graphite), the effect of heating on the structure and capacity of the composite was studied. Subsequent to deposition, the Sn composite material was prepared and heated in air at four different temperatures, namely, 100, 200, 300, and 400°C. Figure 3 presents the XRD results of the composite heated to different temperatures. Based on the XRD data, starting from 200°C, the degree of crystallinity increases with increase in heat-treatment temperature. New peaks appear close to 42 and 46°. No changes in structure are seen at other angles. Nam *et al.*[15] observed that physical vapor deposited SnO_2 is amorphous in nature and when the film was heated, it is converted to crystalline form after 400°C. This is characteristic of electroless deposits also, which are converted to a completely crystalline form after 400°C.[16] According to Kubaschewski and Hopkins,[17] at temperatures below 170°C, the Sn oxides mostly exist in the amorphous state. Tetragonal SnO predominates between 200 and 270°C. Between 280 and 390°C, both SnO and SnO_2 have been observed. Above 390°C, SnO_2 has been found to be the only surface compound under normal pressures. Sn oxides are reduced during the first lithium intercalation reaction based on the following reactions[5]

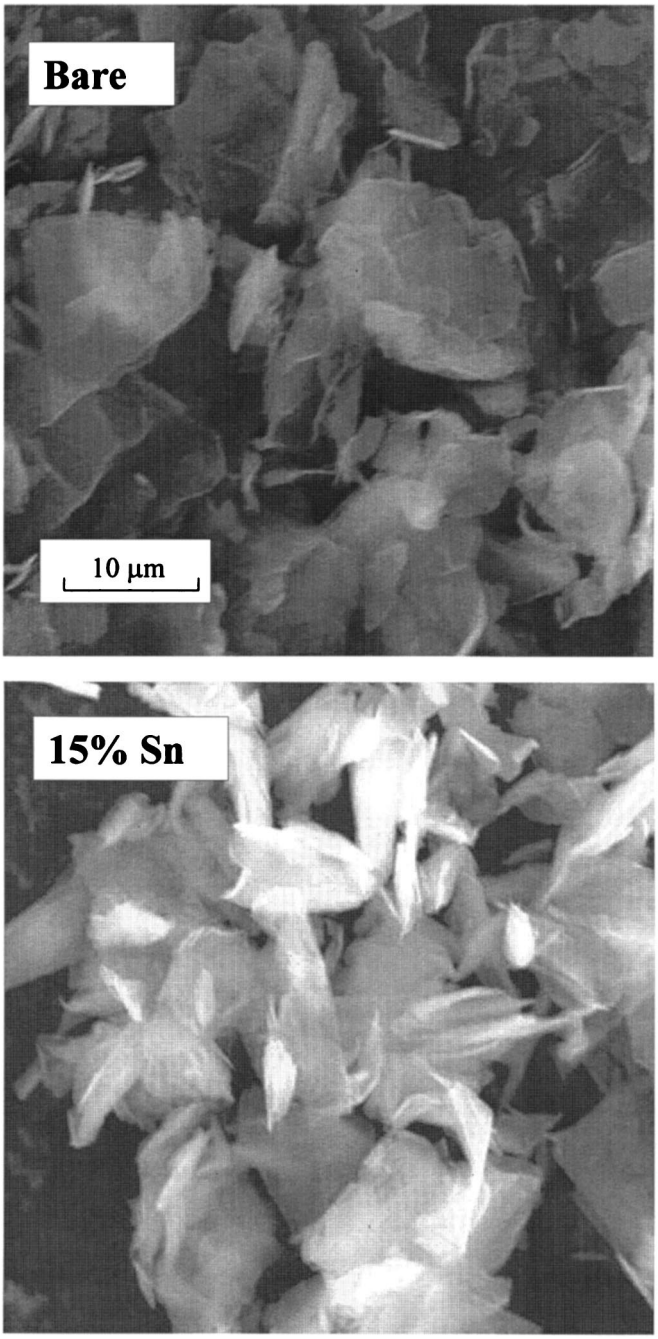

Figure 1. SEM images of (a) bare SFG10 graphite, and (b) 15% Sn on SFG10.

$$6.4Li + SnO \rightarrow Li_2O + Li_{4.4}Sn \quad [1]$$

$$8.4Li + SnO_2 \rightarrow 2Li_2O + Li_{4.4}Sn \quad [2]$$

Downloaded 28 Jul 2011 to 129.252.86.83. Redistribution subject to ECS license or copyright; see http://www.ecsdl.org/terms_use.jsp

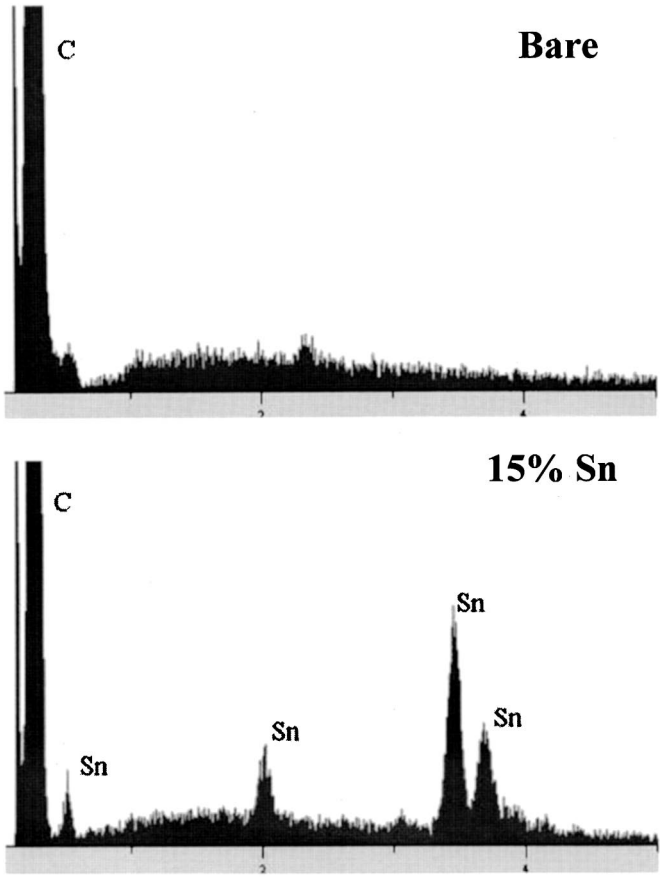

Figure 2. EDAX analysis on bare and 15% Sn-coated SFG10.

These irreversible reactions contribute to the lowering of specific discharge capacity of Sn composite. The amount of lithium consumed in reducing these oxides increases with the increase in oxidation state of Sn. Therefore, samples heat treated at different temperatures can be expected to behave differently in terms of specific discharge capacities.

To study change in composite weight with heating TGA was done on both the bare and 15 wt % Sn on graphite sample in the presence of air. TGA results show a continuous weight loss for the composite. In our case, the underlying substrate graphite oxidizes to CO_2 at temperatures greater than 600°C. Below that temperature, no weight loss is seen for bare graphite. Since Sn oxides are stable up to a temperature of 1000°C, the weight loss for the composite can be attributed to the removal of water.

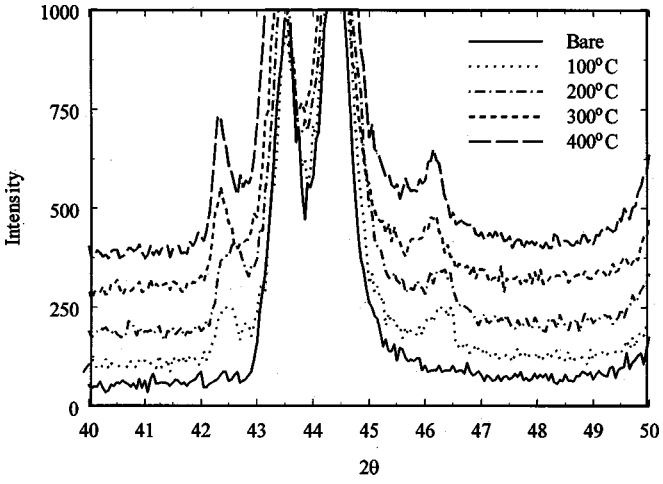

Figure 3. XRD analysis of Sn-coated sample annealed at different temperatures.

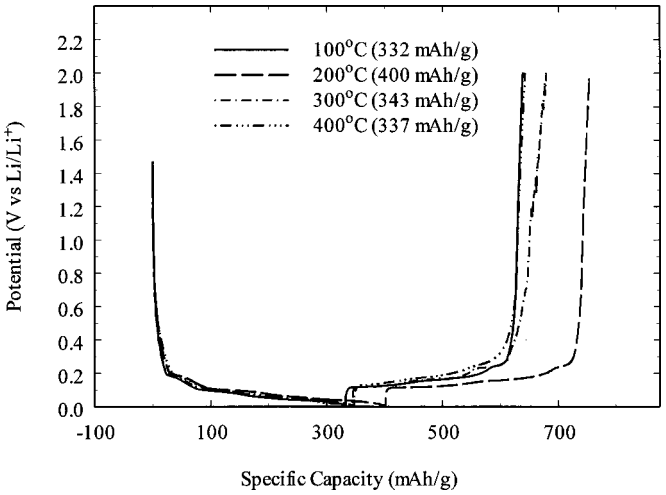

Figure 4. Charge/discharge curves of Sn-coated sample annealed at different temperatures. Cycling was done in 1 M $LiPF_6$ /EC/DMC electrolyte at C/15 rate.

Effect of heating on specific discharge capacity.—Figure 4 shows the charge/discharge studies carried out on the different heat-treated samples at a C/15 rate. According to Courtney and Dahn,[5] during the first discharge lithium bonds to oxygen that was initially bonded to Sn, thereby breaking up the oxide and leaving Sn metal and Li_2O. The rest of the Sn metal can reversibly alloy with Li until the theoretical limit of $Li_{4.4}Sn$. Based on this hypothesis, they observed that the first cycle discharge capacity increased with increase in Sn valence. We observed similar results for the composite material heated to different temperatures. The discharge capacity for the first cycle increased from 701 to 745 mAh/g on heating the sample from 100 to 400°C. This is in accordance with the XRD data, which indicates the formation of crystalline SnO_2 at these temperatures. At 200°C, SnO is the only oxide present and this has a lower discharge capacity in the first cycle. At intermediate temperatures, a mixture of both oxides are present. Due to variation in oxygen content, the discharge capacity changes with temperature of heating.

The specific discharge capacity after 5 cycles was the largest in case of samples heat-treated at 200°C. Lower reversible capacities on heating to higher temperatures can be expected because of the formation of high valence tin oxides. According to Courtney and Dahn,[5] the principal reason for the decline in the capacity observed in the case of tin is the disintegration of the anode material during cycling. According to Idota *et al.*,[8] the ''pulverization'' problems encountered during cycling of the tin material can be greatly reduced by using amorphous tin composite oxides. Lee *et al.*[9] attributed the observed decrease in capacity of a similar graphite-tin composite during cycling to the crystalline nature of the deposited tin material. So, we have surmised that the lower capacities for the composites heated to greater than 200°C, after 5 cycles, are due to the increased crystallinity of the tin material in the composite. The discharge capacity at 100°C was lower than that at 200°C. This is attributed to the presence of water in the composite. For subsequent studies, all composite materials were dried in vacuum at 200°C for 24 h prior to electrode fabrication.

Effect of Sn loading on the specific discharge capacity.—Tin alloys extensively with lithium to form alloys of the form $Li_{22}Sn_5$, which

Downloaded 28 Jul 2011 to 129.252.86.83. Redistribution subject to ECS license or copyright; see http://www.ecsdl.org/terms_use.jsp

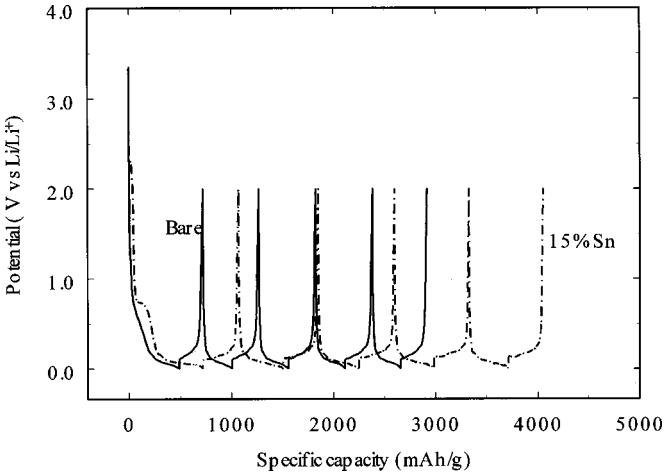

Figure 5. Comparison of charge/discharge curves of bare and 15 wt % Sn-coated graphite. The composite was annealed at 200°C.

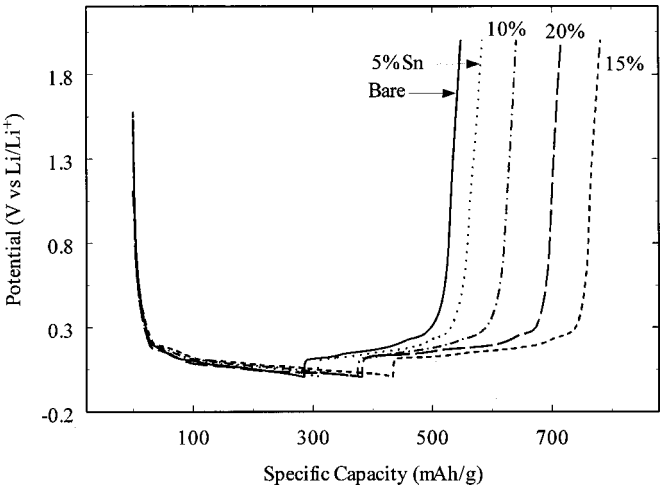

Figure 6. Comparison of charge/discharge curves for composite loaded with different amounts of Sn. Curves for bare SFG10 graphites are also shown for comparison.

gives rise to a theoretical capacity of 991 mAh/g. The reversible reaction of lithium with tin can be given by[5]

$$Li^+ + Sn + e^- \rightarrow Li_xSn \quad (x \leq 4.4)$$

Courtney and Dahn[5] also observed that when tin is used in the pristine form, though it shows a huge initial discharge capacity, it loses it rapidly on cycling due to the cracking and crumbling of the material by the large volume increases that are involved in realizing the lower LiSn alloy phases (Li_5Sn_2, $Li_{13}Sn_5$, Li_7Sn_2, $Li_{22}Sn_5$). They also found that keeping the operating potential window between 1.3 and 0.4 V instead of between 1.3 and 0 V helped in reducing the formation of lower LiSn alloy phases, thereby reducing the capacity loss during cycling.

However, Sn composites prepared by autocatalytic reduction processes possess a stable cycling performance even in the potential range of 0.005 and 2 V *vs.* Li/Li^+. Figure 5 shows the charge/discharge behavior of bare and tin encapsulated SFG10 graphite during the first 5 cycles. Cycling was done at a current density of 0.1 mA/cm^2 corresponding to a C/15 rate. As seen from the plot, Sn composite electrodes possessed higher discharge capacities when compared to that of bare carbon. Also, the capacity retention with cycling was higher in contrast to the observations of Courtney and Dahn.[5] This difference can be attributed to the quasi-crystalline nature and the smaller particle size of the Sn deposits obtained using autocatalytic reduction process. Idota *et al.*[8] observed a similar stable lithium intercalation/deintercalation capacity with cycling in case of amorphous tin composite oxides.

The addition of tin significantly improves the discharge capacity of the composite electrode when compared to that of bare carbon. Figure 6 shows the effect of increasing tin loading on the discharge capacity of the composite. The discharge capacity increases with increase in tin content, reaches a maximunm, and then decreases. The initial increase can be expected due to the increased reaction between tin and lithium. The plot shows that the rise in the specific capacity reaches a maximum at 15 wt % Sn, and the specific discharge capacity begins to decrease with further increase in tin composition. 20% Sn on graphite shows a lower specific capacity of 381.7 mAh/g than that of 15% Sn composite electrodes (433.2 mAh/g). Note that all capacities, unless mentioned, have been normalized to the total weight of the composite. Increasing the tin content beyond 15% can lead to agglomeration of tin, thereby resulting in poor utilization of the tin particles. This could explain the drop in specific capacity with continued increase in Sn content. However, we were not able to acquire SEM data to corroborate our hypothesis that Sn starts to agglomerate beyond 15 wt % in the composite. Figure 7 summarizes the increase in the reversible capacity as a function of the percentage of tin. The graph shows a maximum, thereby indicating the existence of a limit to which tin can be beneficially used to increase the discharge capacity.

Table I presents Sn utilization for various loading of Sn on graphite. As seen from the table, deposition of Sn up to a composition of 15% leads to better utilization of the active material. The reason for this is the fact that increasing the Sn loading results in incorporating more Sn particles on the surface of carbon. This results in a uniform distribution of Sn over a high surface area and hence leads to better utilization. However, increasing the Sn loading further (20 wt %) leads to more tin being coated over the same surface area. This results in layered coatings or agglomerated particles of tin thereby leading to lower utilization of tin. It can be seen that the utilization of Sn remains a constant at around 55% for Sn compositions up to 15 wt %. When the Sn content is increased to 20%, the utilization drops to 31%, suggesting layered deposition of Sn. This was corroborated by the BET surface analysis data that was obtained for various Sn composite materials. BET surface areas for all the Sn composite graphite particles are summarized in Table I. It is seen that the BET surface area of the SnO-C composite decreases with increase in Sn content. The BET surface area of the bare carbon is 9.84 m^2/g. After loading this with 20 wt % Sn, the BET surface

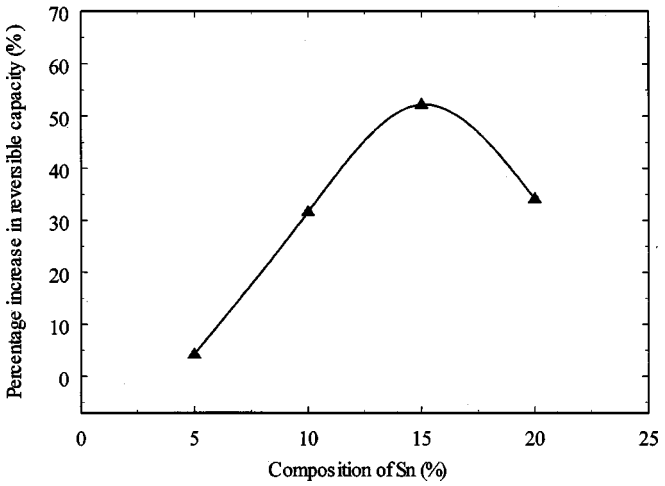

Figure 7. Percentage increase in reversible capacity of the Sn-coated SFG10 samples as a function of Sn loading.

Downloaded 28 Jul 2011 to 129.252.86.83. Redistribution subject to ECS license or copyright; see http://www.ecsdl.org/terms_use.jsp

Table I. Comparison of utilization, surface area, and capacity for Sn-C composite electrodes with different loading of Sn.

Sample	Reversible capacity (mAh/g)	Capacity due to Sn (mAh/g)	Utilization of Sn[a] (%)	Specific surface area (m^2/g)	Volumetric surface area (m^2/cm^3)	Volumetric capacity (mAh/cm^3)
Bare	284.6	···	···	9.84	21.65	626.1
5% Sn	327.8	57.4	55.0	8.52	20.49	788.4
10% Sn	374.6	118.5	53.8	8.30	21.66	977.7
15% Sn	433.2	191.3	54.7	7.61	21.42	1219.5
20% Sn	381.7	154.0	31.1	7.12	21.50	1152.7

[a] Utilization of tin = (Capacity due to tin/weight of tin in the composite)/Theoretical capacity of tin (991 mAh/g) × 100.

area decreases to 7.12 m^2/g. Sn has a much higher bulk density (6.3 g/cm^3) as compared to graphite (2.2 g/cm^3). On loading Sn on carbon, the total weight of the composite increases for a given volume of material, due to the higher density of tin oxide. This results in reducing the BET surface area, as this is normalized to the weight of the material. Table I also shows that the volumetric surface area of the SnO-C composite does not change significantly with increased tin loading. This is to be expected since a small amount of the deposit is dispersed over the large surface of the carbon substrate. While deposition of Sn on graphite increases the weight of the composite no significant change in volume is seen. Hence, the volumetric capacity of the composite electrode increases much more than the specific capacity with increased tin loading as shown in Table I.

As discussed before, Sn oxides undergo a reduction reaction with lithium during the first intercalation step to form Li_2O and Sn. Graphite also undergoes reduction reactions with lithium during the first intercalation cycle leading to the formation of a stable solid electrolyte interphase layer.[18-20] These reduction reactions with Li are irreversible in nature and contribute to a decrease in the specific discharge capacity of the material. Sn-carbon composites will have irreversible capacity losses arising from both the above-mentioned processes. Table II presents the irreversible capacity loss occurring in different Sn composites during the first intercalation cycle. Since the heat-treatment conditions were kept the same for all composites, any difference in the irreversible capacity for the different composites is mainly due to the difference in loading and surface area. The irreversible capacity loss increases with tin loading until a composition of 15 wt % and then decreases for 20 wt %. These results are in agreement with the utilization data presented in Table I. The initial increase in capacity loss can be attributed to the formation of more amount of irreversible Li_2O due to increase in Sn content. As seen previously, increasing Sn loading beyond 15 wt % results in agglomeration of Sn particles. Since the irreversible capacity loss is associated with surface reactions, formation of agglomerates (for 20 wt % Sn) contributes to a lowering of this quantity. Because the irreversible capacity loss of these materials is larger than that of bare graphite, our current research is focused on finding means for reducing this loss.

Electrochemical impedance spectroscopy.—Impedance analysis was carried out on Sn composite and bare carbon electrodes to understand the influence of adding Sn on the ohmic and polarization resistance of the composites. To maintain uniformity, all the impedance studies were done on completely discharged samples (fully lithiated state). Figure 8 shows the Nyquist plots of the composite electrodes. The impedance response in case of Sn-carbon composite is characterized by the presence of two overlapping semicircles followed by a Warburg-type straight line at low frequencies. Aurbach *et al.*[21] have shown that, for carbon anodes, the first semicircle at high frequencies corresponds to the resistance for Li^+ ion migration through the surface films. The second semicircle arises due to double layer charging, and charge transfer resistance. In addition, other factors such as intraparticle electronic resistance and interfacial capacitance may influence the impedance data. In our case, the magnitude of both semicircles decreases with the increased tin loading in the composite. In general, it can be seen that Sn loading leads to a decrease in polarization resistance indicating an improved kinetics in the case of the composites. The magnitude of the high frequency loop for the bare graphite was also significantly higher when compared to that of Sn composite carbon, indicating the lower resistance for Li-ion migration through the surface layer in the case of Sn-coated samples.

Fitting these loops to a semicircle provides information about the polarization resistance value. Careful examination of these impedance curves suggests that the loops, are either depressed semicircles or arcs of semicircles whose center is displaced from the real axis. The data can be compared with the impedance of a plausible electrical equivalent circuit by complex nonlinear least squares fitting to extract parameters (circuit elements) which can be related to physical processes which are likely to be present. Although we typically employ ideal resistors, capacitors, and inductances in an equivalent circuit, actual real elements only approximate ideality over a limited frequency range. In this work, the impedance loops are present as depressed semicircles signifying deviation from ideality. To compensate for this deviation from reality, a distributed phase element was added to the equivalent circuit. Figure 9 shows the electrical equivalent circuit that was used to fit the experimental impedance

Table II. Change in irreversible capacity loss with Sn loading at C/15 rate.

Amount of Sn loading (wt %)	1st cycle discharge capacity (mAh/g)	1st cycle charge capacity (mAh/g)	Irreversible capacity from Sn[a]	Overall irreversible capacity[b] (%)
	485.9	232.7	···	52.1
5	579.2	305.8	60.2	47.2
10	656.0	337.1	100.2	48.6
15	719.6	350.7	115.3	51.3
20	613.3	324.9	70.6	47.0

[a] Irreversible capacity from Sn = Irreversible capacity of the composite; irreversible capacity from graphite.
[b] Overall irreversible capacity = (1st cycle discharge capacity of the sample; 1st cycle charge capacity of the sample)/1st cycle discharge capacity of the sample × 100.

Downloaded 28 Jul 2011 to 129.252.86.83. Redistribution subject to ECS license or copyright; see http://www.ecsdl.org/terms_use.jsp

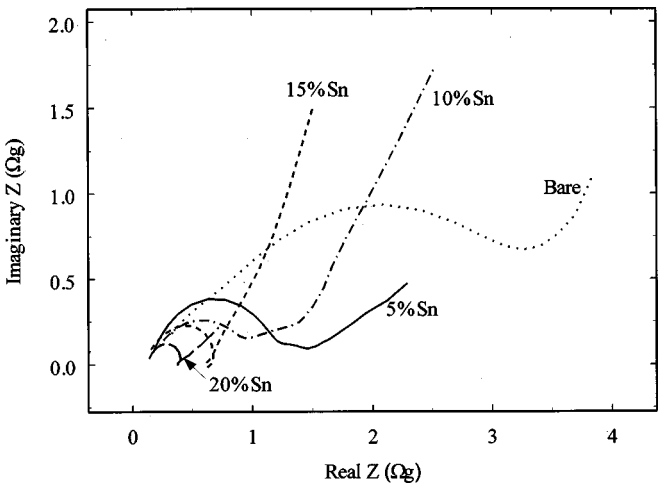

Figure 8. Impedance plots for the bare and Sn-coated SFG10 samples at fully lithiated state.

data. The distributed element used in the equivalent circuit is a Zarc-Cole type wherein a constant phase element (CPE; signifies the semi-infinite noniuniform diffusion occurring in a porous electrode), is placed in parallel with an ideal resistor (reaction resistance). The Zarc produces a complex plane curve, which forms an arc of a circle with center, displaced from the real axis. Further details about the Zarc-Cole fitting and CPE can be obtained from literature.[22]

Table III presents the different resistances for both bare and Sn coated graphite. It can be seen that the bare SFG10 graphite possesses a high polarization resistance value when compared to Sn-encapsulated electrodes. This indicates faster reaction kinetics for the composites as compared to the bare material. The values for the resistance of the surface film is also lower for the composites in comparison to bare graphite. This indicates a lower resistance for the transfer of Li ions through the film. Thus, fitting the experimental data to an equivalent circuit provides information that the improved performance for the Sn coated composites arises from an increase in reaction kinetics and decrease in surface layer resistance.

CVs.—Reversibility and kinetics of Li intercalation in the composite can be studied using CVs. CVs were obtained at a scan rate of 0.05 mV/s. The potential was swept from 1.2 to 0 V *vs.* Li/Li^+ and back to 1.2 V. This potential range is representative of the potential window of the anode under normal battery operating conditions. Figure 10 shows the CV of Sn-encapsulated SFG10 graphite. The CV performed on the bare graphite has also been shown for comparison. Sweeping the potential from 1.2 to 0 V results in lithiating the composite. Kinetics of Li intercalation for both materials remains low till 0.3 V. Beyond this, a sharp increase in the current is seen. According to Dahn *et al.*,[5] cycling bulk SnO between 1.3 and 0.4 V

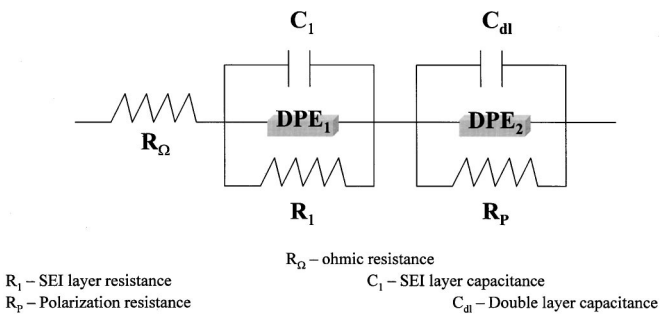

Figure 9. Equivalent electrical circuit used to fit the experimental impedance data.

Table III. Equivalent circuit parameters obtained by fitting the experimental results.

Amount of Sn loading (wt %)	R_Ω (Ω_g)	R_1 (Ω_g)	R_P (Ω_g)
0	0.13	5.0	5.8
5	0.14	0.7	2.0
10	0.14	0.8	0.6
15	0.16	0.8	0.5
20	0.16	0.8	0.5

gives a reversible capacity of approximately 300 mAh/g. In our case, integrating the area under the cathodic curve in Fig. 9 from 1.2 to 0.4 V, gives a charge of 40 mAh/g. This is much lower than that reported by Dahn *et al.*[5] Hence, it is clear that Li alloying with Sn in the composite differs significantly from that reported previously for the bulk material. During deintercalation (sweeping the voltage from 0 to 1.2 V) two characteristic peaks appear at the same voltage for both the bare graphite and the composite. However, the magnitude of the peak current is larger for Sn-coated graphite as compared to the bare material. The plot also shows an increase in the area of the current density-voltage curve for the coated carbon. This serves as an additional support for the increase in the capacity due to tin coating seen in charge/discharge studies. However, no discernible peak corresponding to the reaction of Sn with Li are seen, suggesting that the lithiation reactions with Sn occur in the same potential range as that of carbon. Lower Li-Sn alloy phases (Li_5Sn_2, $Li_{13}Sn_5$, Li_7Sn_2, $Li_{22}Sn_5$) have been observed at a potential range of 0.23-0.10 V.[5] This corresponds to the potential range in which lithiation is seen in the case of the composite. Finally, comparison of the ratio of charges under the anodic and cathodic sweeps reveals a higher coulombic efficiency for the Sn encapsulated sample.

Rate capability studies were done on the samples to ascertain the performance of the materials under varying load conditions. Table IV summarizes the rate capability studies and gives the reversible capacity of the samples at different discharge rates. At an applied load of 0.1 mA/cm^2 (corresponding to a rate of C/15), the bare graphite gives 77% of the theoretical capacity (284.6 mAh/g). As the rate is increased, the performance of the bare graphite decreases. When the rate is increased to C/6, the capacity drops down to 226.3 mAh/g, corresponding to 61% of the theoretical capacity. At even higher rates, the performance of the bare graphite further deteriorates and falls down to a value of 45.2 mAh/g at a 2C rate, giving only 12% of the theoretical capacity. As seen in the impedance stud-

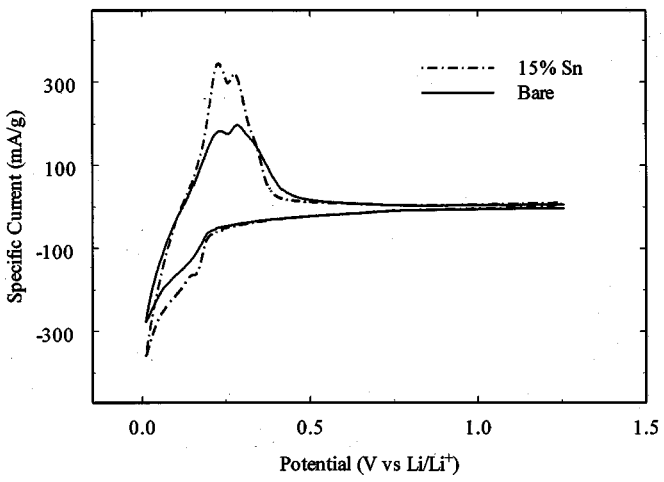

Figure 10. CVs of bare and 15% Sn-coated SFG10 samples in 1 M $LiPF_6$/EC/DMC electrolyte at a scan rate of 0.05 mV/s.

Downloaded 28 Jul 2011 to 129.252.86.83. Redistribution subject to ECS license or copyright; see http://www.ecsdl.org/terms_use.jsp

Table IV. Comparison of rate capability for bare and 15 wt % Sn coated graphite.

	Reversible capacity of the sample (mAh/g)				
Sample	C/15	C/6	C/3	C	2C
Bare	284.6	226.3	128.1	79.1	45.2
15% Sn	433.2	336.6	260.3	198.7	160.5

ies, tin encapsulation decreases the polarization resistance and also improves the conductivity of the composite electrode. Since these parameters play an important role in determining the high rate performance coating graphite with Sn shows significant improvement in the performance of the composite. When the 15% Sn-coated graphite was subjected to rate capability studies it gave a capacity of 433.2 mAh/g at C/15 rate, which far exceeds the theoretical capacity of graphite. However, the utilization of Sn at this rate is only about 55%. Tin utilization does not change much with current until an applied load of C/3 rate. When the rates are increased beyond C/3, the utilization of Sn starts to decrease and reaches a value of 33% at a 2C rate. Still, the specific capacity for the coated sample is higher at any given rate than that for the bare graphite.

Cycle life studies.—Extended charge/discharge studies were carried out to study the cycle life performance of Sn composite and bare graphite anodes. Both electrodes were cycled at a C/15 rate. Figure 11 shows the discharge capacity of the coated and bare graphite over extended cycling. From the plot, we can see that the coated sample displays a constant capacity during cycling. Previous studies[9] on Sn-C composites prepared through a chemical precipitation route show significant loss in capacity for the composite during cycling. This was attributed to large particles of crystalline Sn that crumbled during cycling. On the other hand, Sn when plated over a graphite surface using an autocatalytic reduction procedure gives constant capacity with cycling. In general, the more amorphous the structure is, the better is the utilization and electrochemical stability of the material. Thus, electroless deposition has resulted in incorporation of amorphous tin particles on graphite, which show significant improvement in electrochemical behavior compared to bare SFG10 graphite.

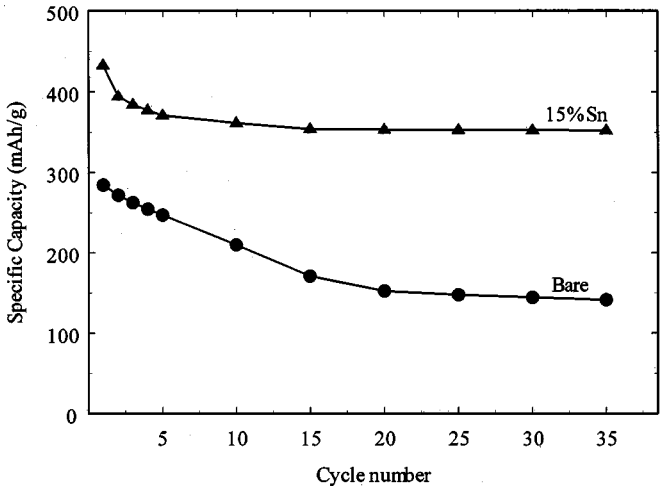

Figure 11. Cycle life studies on bare and 15 wt % Sn coated SFG10 samples at C/15 rate.

Conclusions

Different amounts of Sn were loaded on graphite (Timcal SFG10) by an electroless reduction process to form Sn/C composites. The optimized annealing temperature was found to be 200°C, based on the reversible capacity obtained. A Sn-graphite composite possesses higher capacity and coulombic efficiency, better rate capability, and longer cycle life than the bare SFG10 graphite. Coating of the graphite with Sn reduces the charge-transfer resistance and overall polarization. The Sn-coated samples also showed very good cycling behavior, which has not been observed in previous synthesis of such composite materials.

Acknowledgments

The authors wish to acknowledge the financial support in part by the Department of Energy Division of Chemical Sciences, Office of Basic Energy Sciences, and Sandia National Laboratories, Albuquerque, NM.

The University of South Carolina assisted in meeting the publication costs of this article.

References

1. M. B. Armand, *Material for Advanced Batteries*, D. W. Murphy, J. Broadhead, and B. C. Steele, Editors, p. 145, Plenum Press, New York (1980).
2. D. Guymard and J. M. Tarascon, *J. Electrochem. Soc.*, **139**, 937 (1992).
3. T. Zheng, Q. Zhong, and J. R. Dahn, *J. Electrochem. Soc.*, **142**, L211 (1995).
4. J. Wang, I. D. Raistrick, and R. A. Huggins, *J. Electrochem. Soc.*, **133**, 457 (1986).
5. I. A. Courtney and J. R. Dahn, *J. Electrochem. Soc.*, **144**, 2045 (1997).
6. A. H. Whitehead, J. M. Elliot, and J. R. Owen, *J. Power Sources*, **81-82**, 33 (1999).
7. N. Li and C. Martin, *J. Electrochem. Soc.*, **148**, A164 (2001).
8. Y. Idota, T. Kubota, A. Matsufuji, Y. Maekawa, and T. Miyasaka, *Science*, **276**, 1395 (1997).
9. J. Y. Lee, R. Zhang, and Z. Liu, *J. Power Sources*, **90**, 70 (2000).
10. M. Ramani, B. S. Haran, R. E. White, B. N. Popov, and L. Arsov, *J. Power Sources*, **93**, 209 (2001).
11. P. Yu, J. A. Ritter, R. E. White, and B. N. Popov, *J. Electrochem. Soc.*, **147**, 1280 (2000).
12. P. Yu, B. S. Haran, J. A. Ritter, R. E. White, and B. N. Popov, *J. Power Sources*, **91** 107 (2000).
13. P. W. Wild, *Modern Analysis for Electroplating*, Finishing Publications Ltd., Middlesex, U.K. (1974).
14. P. Yu, J. A. Ritter, R. E. White, and B. N. Popov, *J. Electrochem. Soc.*, **146**, 8 (1999).
15. S. C. Nam, Y. H. Kim, W. I. Cho, B. W. Cho, H. S. Chun, and K. S. Yun, *Electrochem. Solid-State Lett.*, **2**, 9 (1999).
16. G. G. Gawrilov, *Chemical Nickel Plating*, Portcullis Press Ltd., Surrey, England (1979).
17. O. Kubaschewski and B. E. Hopkins, *Oxidation of Metals and Alloys*, Academic Press Inc., London, U.K. (l962).
18. W. Xing and J. R. Dahn, *J. Electrochem. Soc.*, **144**, 1195 (1997).
19. T. Osaka, T. Momma, Y. Matsumoto, and Y. Uchida, *J. Electrochem. Soc.*, **144**, 1709 (1997).
20. F. Kong, J. Kim, X. Song, M. Inaba, K. Kinoshita, and F. McLarnon, *Electrochem. Solid-State Lett.*, **1**, 39 (1998).
21. D. Aurbach, M. D. Levi, E. Levi, H. Teller, B. Markovsky, G. Salitra, U. Heider, and L. Heider, *J. Electrochem. Soc.*, **145**, 3024 (1998).
22. J. R. MacDonald, *Impedance Spectroscopy*, John Wiley & Sons, New York (1987).

Downloaded 28 Jul 2011 to 129.252.86.83. Redistribution subject to ECS license or copyright; see http://www.ecsdl.org/terms_use.jsp